

Current Biology

Estimating the dwarfing rate of an extinct Sicilian elephant

Highlights

- We present mitochondrial genome data from an extinct Mediterranean dwarf elephant
- Dwarf elephant DNA diverged ~0.4 million years ago from the large-bodied ancestor
- Multidisciplinary evidence places a minimum and maximum boundary on dwarfing rate
- We find a size reduction between 0.74 and 200.95 kg and 0.15 and 41.49 mm per generation

Authors

Sina Baleka, Victoria L. Herridge, Giulio Catalano, ..., Kirsty E.H. Penkman, Michael Hofreiter, Johanna L.A. Paijmans

Correspondence

sina.baleka@gmail.com (S.B.),
paijmans.jla@gmail.com (J.L.A.P.)

In brief

Baleka et al. present mitochondrial genome data from an extinct Sicilian dwarf elephant, a small-bodied island lineage that evolved from one of the largest land mammals that ever lived. Combining the genetic data with geochronological and paleontological evidence, Baleka et al. provide an upper and lower estimate of the rate of island dwarfing.

Report

Estimating the dwarfing rate of an extinct Sicilian elephant

Sina Baleka,^{1,2,9,*} Victoria L. Herridge,³ Giulio Catalano,⁴ Adrian M. Lister,³ Marc R. Dickinson,⁵ Carolina Di Patti,⁶ Axel Barlow,⁷ Kirsty E.H. Penkman,⁵ Michael Hofreiter,¹ and Johanna L.A. Paijmans^{1,8,*}

¹Institute for Biochemistry and Biology, University of Potsdam, Karl-Liebknecht-Strasse 24-25, 14476 Potsdam, Germany

²Faculty of Life and Environmental Sciences, University of Iceland, Sæmundargata 2, 101 Reykjavik, Iceland

³Department of Earth Sciences, Natural History Museum, Cromwell Road, London SW7 5BD, UK

⁴Dipartimento di Scienze e Tecnologie Biologiche, Chimiche e Farmaceutiche, Laboratory of Anthropology, Università degli Studi di Palermo, 90128 Palermo, Italy

⁵Department of Chemistry, University of York, Heslington, York YO10 5DD, UK

⁶Museo Geologico “G.G. Gemmellaro” - Università degli Studi di Palermo, Corso Tukory 131, 90133 Palermo, Italy

⁷School of Science and Technology, Nottingham Trent University, Clifton Lane, Nottingham NG11 8NS, UK

⁸Present address: Department of Zoology, University of Cambridge, Downing Street, Cambridge CB2 3EJ, UK

⁹Lead contact

*Correspondence: sina.baleka@gmail.com (S.B.), paijmans.jla@gmail.com (J.L.A.P.)

<https://doi.org/10.1016/j.cub.2021.05.037>

SUMMARY

Evolution on islands, together with the often extreme phenotypic changes associated with it, has attracted much interest from evolutionary biologists. However, measuring the rate of change of phenotypic traits of extinct animals can be challenging, in part due to the incompleteness of the fossil record. Here, we use combined molecular and fossil evidence to define the minimum and maximum rate of dwarfing in an extinct Mediterranean dwarf elephant from Puntali Cave (Sicily).¹ Despite the challenges associated with recovering ancient DNA from warm climates,² we successfully retrieved a mitogenome from a sample with an estimated age between 175,500 and 50,000 years. Our results suggest that this specific Sicilian elephant lineage evolved from one of the largest terrestrial mammals that ever lived³ to an island species weighing less than 20% of its original mass with an estimated mass reduction between 0.74 and 200.95 kg and height reduction between 0.15 and 41.49 mm per generation. We show that combining ancient DNA with paleontological and geochronological evidence can constrain the timing of phenotypic changes with greater accuracy than could be achieved using any source of evidence in isolation.

RESULTS AND DISCUSSION

Evolution on islands is a process that can lead to a variety of phenotypic changes in a relatively short time span, including dwarfing and gigantism.⁴ Investigating the rate of these phenotypic changes provides insights into the speed and flexibility of adaptation to a novel environment. Accurate measurement of this change, however, is challenging. The exact timing of colonization of the island is often uncertain, as the fossil record is incomplete and often challenging to date with accuracy. Furthermore, there are cases where the ancestral state of the colonizing individuals is unknown. Molecular dating can provide a means to measure the rate of evolutionary change, as it allows for an estimation of the time to the common ancestor of the lineages under investigation. However, for the multitude of island dwarfs and giants that are now extinct, applying such approaches is hampered by suboptimal climatic conditions for DNA survival, as many islands where such processes took place are located at low latitudes.^{5,6} The mammalian petrous bone has been shown to preserve endogenous DNA better than other skeletal elements^{7,8} and may therefore represent the preferred material for samples from challenging preservation conditions. Similarly,

despite its inherent limitations, mitochondrial DNA remains the marker of choice for DNA studies on samples from challenging preservation conditions due to its high number of copies per cell.^{9,10} Here, we have overcome the challenges associated with DNA preservation in low latitude regions by sampling the petrous bone of a Sicilian dwarf elephant. We reconstruct its mitochondrial genome sequence and use the data to estimate the dwarfing rate for this lineage.

Sicilian dwarf elephants are excellent examples of the extreme morphological changes that island evolution can effectuate (Figure 1). Current common usage distinguishes at least two taxa that existed in the last one million years, delineated on the basis of size: the 1 m tall *Palaeoloxodon falconeri*, and the stratigraphically younger 2 m tall *Palaeoloxodon cf. mnaidriensis* (see STAR Methods for additional details).^{11,12} The faunal history of the Sicilian Pleistocene suggests several faunal turnover events, and the exact number of dwarf elephant taxa represented in the fossil record is an ongoing debate (STAR Methods).^{1,13} Our specimen has been tentatively assigned to *P. cf. mnaidriensis*. However, since the taxonomy of Sicilian dwarf elephants is subject to discussion, we refer to it here as the “Puntali elephant” (STAR Methods). Nevertheless, there is broad consensus that all

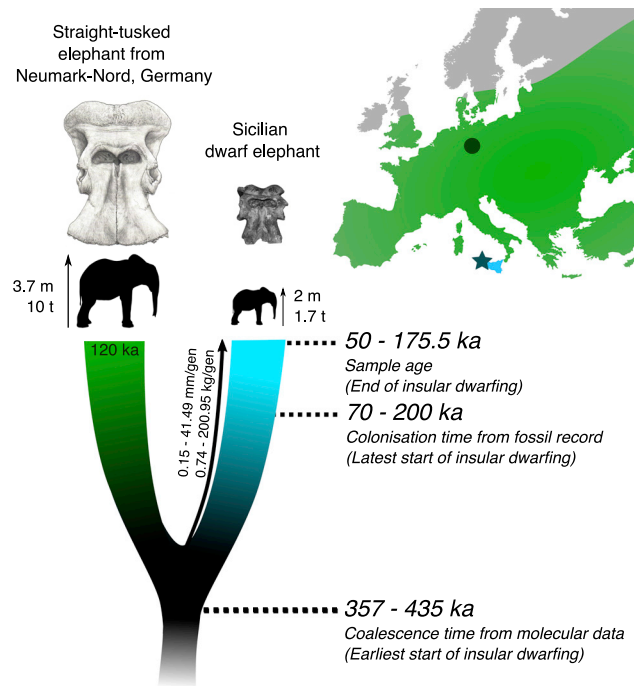


Figure 1. Phylogenetic relationship between the Puntali dwarf elephant and the straight-tusked elephant *Palaeoloxodon antiquus*
Schematic diagram depicting the hypothesized models of insular dwarfing. The crania are displayed to scale, showing the reconstruction of a skull from Neumark-Nord, Germany,¹⁷ and skull GP4 from Puntali cave,¹ displaying the large change in size caused by insular evolution. The inset map displays the distribution of straight-tusked elephants in Europe in green, as well as the site of the previously sampled specimens from Neumark-Nord in Germany (dark green dot). The island of Sicily and the approximate sampling site of Puntali are indicated in blue and with a star, respectively. See also Table S3.

elephant material found on Sicily is attributable to the genus *Palaeoloxodon*, and it is hypothesized that the Puntali elephant, with its estimated shoulder height of 2 m, was a direct descendant of the European straight-tusked elephant *Palaeoloxodon antiquus*, estimated at 3.7 m in height with a mass of 10 tonnes (STAR Methods), that occurred on the European mainland during the Pleistocene between 800 and 40 ka (thousand years ago; Figure 1).^{14,15} The ancestor of the Puntali elephant is suggested to have colonized Sicily from mainland Europe around 200 ka,¹³ although multiple colonization and dwarfing events of different elephant lineages on Sicily can complicate this estimate.¹⁶

We define the age of the Puntali specimen as the end of the dwarfing process, although the actual dwarfing process could have been completed earlier.^{18,19} Several different ages have been proposed for the Puntali material based on biostratigraphic indicators (147 ± 28.7 ka, 88 ± 19.5 ka, and 70–20 ka; STAR Methods). In order to test these, we performed acceleration mass spectrometry radiocarbon dating of the Puntali specimen used for DNA analysis. The sample proved to be beyond the range of radiocarbon dating, leading to a minimal age estimation of approximately 50 ka (STAR Methods). We therefore also applied amino acid geochronology dating, which is a relative dating method based on comparing the extent of intra-crystalline protein degradation to that of material of known age. The intra-crystalline

protein degradation data from the tooth enamel of the Puntali elephant was compared with data from additional dwarf elephant material from Puntali and a second Sicilian site (Spinagallo; Table S1), as well as recently published elephantid material from the UK.²⁰ The intra-crystalline protein degradation in enamel from the Puntali elephant, as well as other specimens from Puntali, is considerably lower than that observed in material from Spinagallo, which has been dated to ~230–350 ka (Figure S1).²¹ Moreover, the material from Puntali Cave shows intra-crystalline protein degradation similar to material from Crayford, UK, which has been correlated with marine oxygen isotope stage (MIS) 6/7 (~200 ka).^{22,23} As the rate of intra-crystalline protein degradation will be faster at the higher temperatures in Sicily compared to the UK, the Puntali material should be younger than the Crayford material, supporting an age estimate younger than 200 ka (STAR Methods), in line with a colonization event during MIS 6. However, as only a limited comparative dataset is available, the intra-crystalline protein degradation is currently not able to provide a more accurate age estimate. As additional intra-crystalline protein degradation data for fossil material from southern Europe becomes available, it should become possible to provide a narrower age constraint for the Puntali elephant. Together, the amino acid geochronology, radiocarbon dating and the previously published electron spin resonance (ESR) dating²⁴ bracket the age of the Puntali sample between 175.5 and 50 ka and present an additional line of evidence confirming the biostratigraphical age estimation of the Puntali elephant (STAR Methods).

The divergence time from the Puntali elephant's closest mainland relative can be seen as the earliest possible start of the dwarfing process, assuming that their common ancestor was a full-sized straight-tusked elephant (e.g., see Erkek and Lister²⁵ for sizes of Italian mainland straight-tusked elephants). This thus offers a second estimate of the onset of dwarfing for the Puntali lineage, independent from fossil evidence. To investigate the divergence time from the mainland lineage, we recovered mitochondrial sequences from a Puntali elephant petrous bone to assemble its mitochondrial genome to 95.5% completion with an average read depth of $61 \times$ (STAR Methods; Figure S2). Phylogenetic analysis of extinct and extant elephants places the Puntali elephant as sister to the straight-tusked elephant lineage recovered from Neumark-Nord, Germany, with high support (100% bootstrap support, 1.0 Bayesian posterior probability; Figures 2, S2, and S3). Using a fossil-calibrated Bayesian Skyline Population model in BEAST,²⁶ we find the estimated mean coalescence time between the Puntali elephant and the straight-tusked elephant mitogenomes from Neumark-Nord to be 402 ka using the minimum sample age (50 ka; 95% credibility interval: 283–531 ka) to 435 ka using the maximum sample age (175.5 ka; 95% credibility interval: 320–564 ka; STAR Methods). These ages closely align with the mean divergence time when applying a speciation model (357 ka for a sample age of 50 ka [95% credibility interval: 249–476 ka] to 398 ka for a sample age of 175.5 ka [95% credibility interval: 293–511 ka]; Figure 2, inset; STAR Methods). Since gene-lineage coalescence always pre-dates population separation (assuming no post-divergence gene flow), this coalescence time thus represents the maximum age for the colonization of Sicily by the Puntali elephant lineage. Post-divergence gene flow between species could lead to paraphyly in the mitochondrial phylogeny, which has previously been

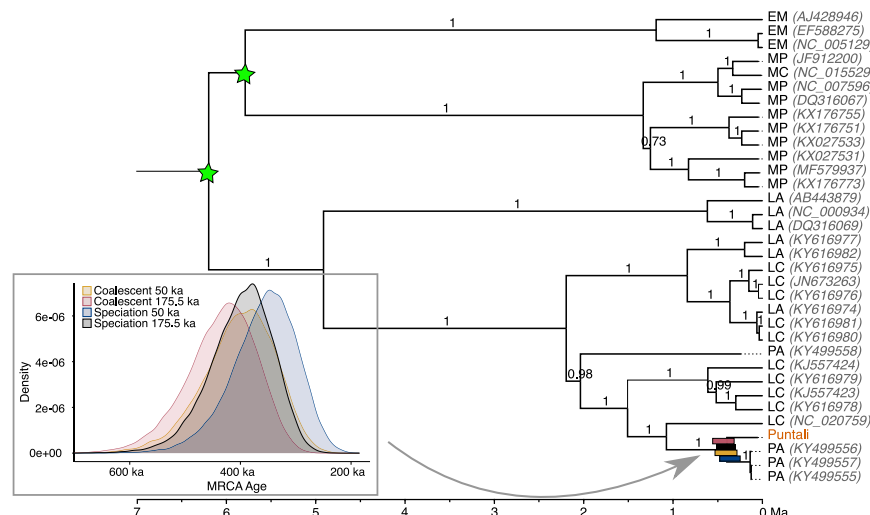


Figure 2. Calibrated Bayesian phylogeny of 34 complete elephant mitochondrial genomes

Calibrated nodes are indicated with a star. Node support is given as Bayesian posterior probability. EM, *Elephas maximus* (Asian elephant); MP, *Mammuthus primigenius* (Woolly mammoth); MC, *Mammuthus columbi* (Columbian mammoth); LA, *Loxodonta africana* (African savanna elephant); LC, *Loxodonta cyclotis* (African forest elephant); PA, *Palaeoloxodon antiquus* (European straight-tusked elephant). The inset shows density distribution of divergence times for different sample ages and tree priors. See also Figures S2 and S3 and Table S2.

reported for the two extant African elephant species^{27,28} and thus complicate the interpretation of divergence times between populations. Although we find no evidence of mitochondrial paraphyly involving Puntali, Neumark-Nord straight-tusked elephants and African elephants in the complete mitogenomes (Figures 2 and S2), or short mtDNA sequences (Figure S3), the analyses of additional samples and nuclear markers will be required to confirm that the mitochondrial relationships we recover between the Puntali and Neumark-Nord straight-tusked elephants corresponds to the species tree.

The actual source population for the colonization of Sicily was most likely located in mainland Italy. The estimated coalescence time based on a more northerly German population may well represent the split between these regional populations of mainland straight-tusked elephants, rather than the divergence of the Puntali elephant from its mainland ancestor. In mainland Europe, the straight-tusked elephant fossils display high variability in cranial morphology, which has led to some debate whether these differences should be considered as indicative of distinct northern and southern subspecies, or even species.^{29–32} Although the mitochondrial DNA places the Puntali and Neumark-Nord elephants as sister lineages, the skull morphology of the Puntali elephant is similar to the southern populations,¹ whereas the Neumark-Nord elephants display the cranial characteristics of the northern straight-tusked elephant populations.³⁰ However, because of the non-monophyletic nature of straight-tusked elephant mitochondrial genomes sequenced to date, and the absence of additional sequences from fossils of which the cranial morphology can be determined, it is unknown if the coalescence time between these lineages represents the divergence between the northern and southern straight-tusked elephant populations. More thorough sampling of European straight-tusked elephants is required to further investigate the population structure within the straight-tusked elephant as well as the colonization dynamics of southern European islands. The molecular divergence estimate between Puntali and mainland straight-tusked elephants should thus be primarily considered an absolute upward constraint on the onset of dwarfing, leading to a minimum dwarfing rate.

The latest possible onset of the dwarfing process can only be constrained on the basis of the age of the first documented small-bodied Puntali elephant lineage on Sicily, which continues to be controversial. This age can be considered an absolute lower constraint to the onset of dwarfing, as the Puntali elephant lineage at this point has already gone through (at least part of) its dwarfing process,³³ highlighting the value of a multidisciplinary estimation of the dwarfing rate. Colonization of Sicily from mainland Europe is likely to have occurred during climate intervals that are accompanied by low sea levels (glacials), due to reduced sea barriers and/or land bridge connections. Although elephants are able to swim, making a landbridge not a requirement for colonization,³⁴ lower sea levels would make colonization more likely. It has been suggested that the ancestor of the Puntali elephant colonized Sicily around 200 ka at the earliest,¹ consistent with the onset of the MIS 6 sea level drop at ~200 ka, with the lowest levels estimated to be around 160–140 ka.³⁵ Due to uncertainty about the age of the Puntali material, we also considered the onset of rapid sea level drop at the end of MIS5e (~125 ka) and the low sea level during MIS4 (~70 ka) as possible colonization dates (Table 1).

Using the youngest and oldest estimates for the age of the Puntali elephant, and the most upward and bottom constraints of the start of dwarfing, we can provide minimum and maximum estimates of the average dwarfing rate of the Puntali elephant lineage. The intermediate potential scenarios using intermediate sample ages and alternative onsets of dwarfing are listed in Table 1. Size and body mass reduction were calculated assuming shoulder height and body mass for the straight-tusked elephant of 3.7 m and 10 t, and 2 m and 1.7 t for Puntali elephants (STAR Methods). We present both the dwarfing rate per year and per generation. As generation time for the straight-tusked elephants, we are utilizing that of a closely related extant species, the African savanna elephant (31 years), following previous publications.^{36,37} This likely represents a maximum estimate: generation time may have decreased over time for the Sicilian dwarf elephant, as body mass and generation time are generally correlated.³⁸ The dwarfing rate is thus calculated by dividing the total amount of dwarfing divided by the total time. The resulting upper and lower potential dwarfing rates for the Puntali dwarf elephant are a body mass reduction between 0.02 and 6.48 kg per year, and a reduction of shoulder height between 0.005 and

Table 1. Outline of different possible dwarfing times

Sample age	Colonization date				Divergence time	
	70 ka	125 ka	140 ka	200 ka	357/402 ka	398/435 ka
	lowest sea level during MIS 4	start of sea level drop end of MIS 5e	lowest sea level MIS 6	start of sea level drop MIS 6	Bayesian divergence time range using youngest possible sample age (=50 ka)	Bayesian divergence time range using oldest possible sample age (=175.5 ka)
50 ka (youngest possible age based on carbon dating)	20 ka	75 ka	90 ka	150 ka	307/352 ka	–
68.7 ka (lower bound of ESR EU model)	1.3 ka	56.3 ka	71.3 ka	131.3 ka	–	–
88.2 ka (mean ESR EU age 88.2 ± 19.5ka)	–	36.8 ka	51.8 ka	111.8 ka	–	–
107.7 ka (upper bound of ESR EU model)	–	17.3 ka	32.3 ka	92.3 ka	–	–
118.1 ka (lower bound of ESR LU model)	–	6.9 ka	21.9 ka	81.9 ka	–	–
146.8 ka (mean ESR LU age 146.8 ± 28.7 ka)	–	–	–	53.2 ka	–	–
175.5 ka (upper bound of ESR LU model)	–	–	–	24.5 ka	–	222.5/259.5 ka

Using all potential sample ages of the Puntali specimen, potential colonization dates of Sicily of the Puntali elephant lineage, and fossil-calibrated molecular divergence times (using youngest and oldest possible sample age and a speciation/coalescent prior, respectively) from the closest full-sized relative, we calculate all possible lengths of the dwarfing process. The longest and shortest dwarfing intervals are highlighted in bold. See also [Figure S1](#) and [Table S1](#).

1.34 mm per year—corresponding to 0.74–200.95 kg and 0.15–41.49 mm per generation. In order to place these evolutionary rates into context, they were converted to haldanes, a unit of rates where one haldane corresponds to a change in trait by one standard deviation per generation.^{39,40} This method corrects for the sampling interval, so despite encompassing a wide range of time over which dwarfing may have occurred (from 352 to 1.3 ka; [Table 1](#)), calculated rates for the shoulder height and body mass fall within other observed paleontological evolutionary rates, at the upper (i.e., fast) end of the range (Figure 8 in Gingerich;⁴⁰ [STAR Methods](#)). Moreover, the magnitude of dwarfing resulting from this rapid evolutionary process was truly striking, as it resulted in a loss of body mass of almost 85% in one of the largest terrestrial mammals that ever lived.

Conclusions

Evolution on islands is often seen as one of the most striking examples of “evolution in action,” and as descendants of giants, the extinct dwarf elephants are among the most intriguing examples of insular evolution. To put the extent of size reduction the Puntali elephant has undergone into context, it would be comparable to modern humans dwarfing to approximately the size of a Rhesus macaque. However, constraining the time span of dwarf elephant evolution using molecular dating is particularly difficult, as ancient DNA does not survive well in the warm climates they lived in. Here, we have overcome the challenges associated with retrieving Pleistocene DNA from a Mediterranean island and provide a first molecularly and biochronologically calibrated range for dwarfing rates of an insular species. The reconstruction of ancient nuclear genomes, although presenting a significant

challenge for Pleistocene specimens from warm climates, would be required to overcome the inherent limitations of mitochondrial DNA as a single marker, and could further allow identification and investigation of functional regions under selection in the dwarfing process as well as the exceptional hybrid origin of the straight-tusked elephant.³⁷

STAR★METHODS

Detailed methods are provided in the online version of this paper and include the following:

- [KEY RESOURCES TABLE](#)
- [RESOURCE AVAILABILITY](#)
 - Lead contact
 - Materials availability
 - Data and code availability
- [EXPERIMENTAL MODEL AND SUBJECT DETAILS](#)
 - Samples
 - Taxonomy of Sicilian dwarf elephants
 - Faunal complex correlations and age of sample
- [METHOD DETAILS](#)
 - Laboratory procedures
- [QUANTIFICATION AND STATISTICAL ANALYSIS](#)
 - Bioinformatic procedures

SUPPLEMENTAL INFORMATION

Supplemental information can be found online at <https://doi.org/10.1016/j.cub.2021.05.037>.

ACKNOWLEDGMENTS

This project received funding from the European Research Council (consolidator grant GeneFlow no. 310763 to M.H.), the Quaternary Research Association, and NERC (NE/K500987/1, NE/F01824X/1, and NE/S010211/1). We thank Matthias Meyer for providing capture baits and Sheila Taylor for technical support in the amino acid analyses. We would like to thank Rossana Sanfilippo, Antonietta Rosso, Francesco Sciuto, Laura Bonfiglio, and Gianni Insacco for their expertise and help with obtaining additional enamel samples for comparison. We would also like to thank Marco Ferretti for the high quality picture of the Puntali Elephant skull GP4.

AUTHOR CONTRIBUTIONS

Conceptualization, M.H., G.C., and S.B.; methodology, M.H., S.B., and J.L.A.P.; investigation, S.B., J.L.A.P., A.B., and M.R.D.; formal analysis, S.B., J.L.A.P., M.H., A.B., A.M.L., V.L.H., M.R.D., and K.E.H.P.; writing – original draft, S.B. and J.L.A.P.; writing – review & editing, S.B., V.L.H., A.B., G.C., M.R.D., A.M.L., K.E.H.P., M.H., and J.L.A.P.; resources, G.C. and C.D.P.; visualization, S.B. and J.L.A.P.; supervision, M.H., J.L.A.P., A.M.L., K.E.H.P., and A.B.

DECLARATION OF INTERESTS

The authors declare no competing interests.

Received: January 7, 2020

Revised: March 29, 2021

Accepted: May 17, 2021

Published: June 18, 2021

REFERENCES

1. Ferretti, M.P. (2008). The dwarf elephant *Palaeoloxodon mnaidriensis* from Puntali Cave, Carini (Sicily; late Middle Pleistocene): anatomy, systematics and phylogenetic relationships. *Quat. Int.* 182, 90–108.
2. Hofreiter, M., Pajmians, J.L.A., Goodchild, H., Speller, C.F., Barlow, A., Fortes, G.G., Thomas, J.A., Ludwig, A., and Collins, M.J. (2015). The future of ancient DNA: technical advances and conceptual shifts. *BioEssays* 37, 284–293.
3. Larramendi, A. (2016). Shoulder height, body mass, and shape of proboscideans. *Acta Palaeontol. Pol.* 61, 537–574.
4. Foster, J.B. (1964). Evolution of mammals on islands. *Nature* 202, 234–235.
5. Kehlmaier, C., Barlow, A., Hastings, A.K., Vamberger, M., Pajmians, J.L.A., Steadman, D.W., et al. (2017). Tropical ancient DNA reveals relationships of the extinct Bahamian giant tortoise *Chelonoidis alburyorum*. *Proc. Biol. Sci.* 284, 20132235.
6. Woods, R., Turvey, S.T., Brace, S., MacPhee, R.D.E., and Barnes, I. (2018). Ancient DNA of the extinct Jamaican monkey *Xenothrix* reveals extreme insular change within a morphologically conservative radiation. *Proc. Natl. Acad. Sci. USA* 115, 12769–12774.
7. Gamba, C., Jones, E.R., Teasdale, M.D., McLaughlin, R.L., González-Forbes, G., Mattiangeli, V., Domboróczki, L., Kóvári, I., Pap, I., Anders, A., et al. (2014). Genome flux and stasis in a five millennium transect of European prehistory. *Nat. Commun.* 5, 5257.
8. Pinhasi, R., Fernandes, D., Sirak, K., Novak, M., Connell, S., Alpaslan-Roodenberg, S., Gerritsen, F., Moiseyev, V., Gromov, A., Raczyk, P., et al. (2015). Optimal ancient DNA yields from the inner ear part of the human petrous bone. *PLoS ONE* 10, e0129102.
9. Pajmians, J.L.A., Barnett, R., Gilbert, M.T.P., Zepeda-Mendoza, M.L., Reumer, J.W.F., de Vos, J., Zazula, G., Nagel, D., Baryshnikov, G.F., Leonard, J.A., et al. (2017). Evolutionary history of saber-toothed cats based on ancient mitogenomics. *Curr. Biol.* 27, 3330–3336.e5.
10. Westbury, M., Baleka, S., Barlow, A., Hartmann, S., Pajmians, J.L.A., Kramarz, A., et al. (2017). A mitogenomic timetree for Darwin's enigmatic South American mammal *Macrauchenia patachonica*. *Nat. Commun.* 8, 15951.
11. Burgio, E., and Cani, M. (1988). Sul ritrovamento di elefanti fossili ad Alcamo (Trapani, Sicilia). *Nat. Sicil.* 12, 87–97.
12. Bada, J.L., Belluomini, G., Bonfiglio, L., Branca, M., Burgio, E., and Delitala, L. (1991). Isoleucine epimerization ages of Quaternary mammals from Sicily. *Quat.* 4, 49–54.
13. Herridge, V.L. (2010). Dwarf elephants on Mediterranean islands: a natural experiment in parallel evolution, Volume 1 and 2 (University College London), Doctoral dissertation.
14. Lister, A.M. (2016). Dating the arrival of straight-tusked elephant (*Palaeoloxodon* spp.) in Eurasia. *Bull. Mus. Anthropol. Prehist. Monaco* 6 (Suppl.), 123–128.
15. Stuart, A.J. (2005). The extinction of woolly mammoth (*Mammuthus primigenius*) and straight-tusked elephant (*Palaeoloxodon antiquus*) in Europe. *Quat. Int.* 126–128, 171–177.
16. Palombo, M.R. (2018). Insular mammalian fauna dynamics and paleogeography: a lesson from the Western Mediterranean islands. *Integr. Zool.* 13, 2–20.
17. Schauer, K. (2010). Wie sahen sie aus? Zur Rekonstruktion des *Palaeoloxodon antiquus* aus den Seeablagerungen von Neumark-Nord. In *Elefantenreich - Eine Fossile Welt in Europa*, H. Meller, ed. (Landesamt für Denkmalpflege und Archäologie Sachsen-Anhalt – Landesmuseum für Vorgeschichte Halle).
18. Lister, A.M. (1993). “Gradualistic” evolution: its interpretation in Quaternary large mammal species. *Quat. Int.* 19, 77–84.
19. Diniz-Filho, J.A.F., Jardim, L., Rangel, T.F., Holden, P.B., Edwards, N.R., Hortal, J., Santos, A.M.C., and Raia, P. (2019). Quantitative genetics of body size evolution on islands: an individual-based simulation approach. *Biol. Lett.* 15, 20190481.
20. Dickinson, M.R., Lister, A.M., and Penkman, K.E.H. (2019). A new method for enamel amino acid racemization dating: a closed system approach. *Quat. Geochronol.* 50, 29–46.
21. Richards, D., Herridge, V.L., Nita, D., Schwenninger, J.-L., Lister, A., Mangano, G., and Bonfiglio, L. (2019). Constraining the chronology of dwarf elephant evolution using Quaternary deposits in coastal caves of the Mediterranean. In *20th Congress of the International Union for Quaternary Research*.
22. Schreve, D.C. (2001). Differentiation of the British late Middle Pleistocene interglacials: the evidence from mammalian biostratigraphy. *Quat. Sci. Rev.* 20, 1693–1705.
23. Bridgland, D.R. (2014). Lower Thames terrace stratigraphy: latest views. In *The Quaternary of the Lower Thames & Eastern Essex Field Guide*, D.R. Bridgland, P. Allen, and T.S. White, eds. (Quaternary Research Association), pp. 1–10.
24. Rhodes, E.J. (1996). ESR dating of tooth enamel. In *Siracusa: Le ossa dei giganti: lo scavo paleontologico di Contrada Fusco*, B. Basile, and S. Chialdi, eds. (Arnaldo Lombardi Promozione), pp. 39–44.
25. Erkek, E.E., and Lister, A.M. (2021). The skeleton of a straight-tusked elephant, *Palaeoloxodon antiquus* (Falconer and Cautley, 1847) from Selsey, England, and growth and variation in *Palaeoloxodon* of the European Pleistocene. *J. Quat. Sci.* 36, 211–223. Published online February 18, 2021. <https://doi.org/10.1002/jqs.3277>.
26. Stadler, T., and Yang, Z. (2013). Dating phylogenies with sequentially sampled tips. *Syst. Biol.* 62, 674–688.
27. Roca, A.L., Georgiadis, N., and O'Brien, S.J. (2007). Cyto-nuclear genomic dissociation and the African elephant species question. *Quat. Int.* 169–170, 4–16.
28. Brandt, A.L., Ishida, Y., Georgiadis, N.J., and Roca, A.L. (2012). Forest elephant mitochondrial genomes reveal that elephantid diversification in Africa tracked climate transitions. *Mol. Ecol.* 21, 1175–1189.
29. Saegusa, H., and Gilbert, W.H. (2008). Elephantidae. In *Homo erectus in Africa, Pleistocene Evidence From the Middle Awash*, W.H. Gilbert, and B. Asfaw, eds. (Univ. of California Press), pp. 193–226.

30. Larramendi, A., Palombo, M.R., and Marano, F. (2017). Reconstructing the life appearance of a Pleistocene giant: size, shape, sexual dimorphism and ontogeny of *Palaeoloxodon antiquus* (Proboscidea: Elephantidae) from Neumark-Nord 1 (Germany). *Boll. Soc. Paleontol. Ital.* 56, 299–317.
31. Larramendi, A., Zhang, H., Palombo, M.R., and Ferretti, M.P. (2020). The evolution of *Palaeoloxodon* skull structure: Disentangling phylogenetic, sexually dimorphic, ontogenetic, and allometric morphological signals. *Quat. Sci. Rev.* 229, 106090.
32. Palombo, M.R. (2010). The straight-tusked elephants from Neumark-Nord. A glance into a lost world. In *Elefantenreich – Eine Fossilwelt in Europa*, H. Meller, ed. (Landesamt für Denkmalpflege und Archäologie Sachsen-Anhalt – Landesmuseum für Vorgeschichte Halle), pp. 219–247.
33. Bonfiglio, L., and Berdar, A. (1983). Gli elefanti del Pleistocene superiore di Archi (Reggio Calabria). Nuove evidenze di insularità della Calabria meridionale durante il ciclo Tirreniano. *Boll. Soc. Paleontol. Ital.* 25, 9–34.
34. Johnson, D.L. (1980). Problems in the land vertebrate zoogeography of certain islands and the swimming powers of elephants. *J. Biogeogr.* 7, 383–398.
35. Spratt, R.M., and Lisiecki, L.E. (2016). A Late Pleistocene sea level stack. *Clim. Past* 12, 1079–1092.
36. Rohland, N., Reich, D., Mallick, S., Meyer, M., Green, R.E., Georgiadis, N.J., Roca, A.L., and Hofreiter, M. (2010). Genomic DNA sequences from mastodon and woolly mammoth reveal deep speciation of forest and savanna elephants. *PLoS Biol.* 8, e1000564.
37. Palkopoulou, E., Lipson, M., Mallick, S., Nielsen, S., Rohland, N., Baleka, S., Karpinski, E., Ivancevic, A.M., To, T.-H., Kortschak, R.D., et al. (2018). A comprehensive genomic history of extinct and living elephants. *Proc. Natl. Acad. Sci. USA* 115, E2566–E2574.
38. Damuth, J., and MacFadden, B.J. (1990). *Body Size in Mammalian Paleobiology: Estimation and Biological Implications* (Cambridge University Press).
39. Gingerich, P.D. (1993). Quantification and comparison of evolutionary rates. *Am. J. Sci.* 293A, 453–478.
40. Gingerich, P.D. (2001). Rates of evolution on the time scale of the evolutionary process. *Genetica* 112–113, 127–144.
41. Gansauge, M.-T., and Meyer, M. (2013). Single-stranded DNA library preparation for the sequencing of ancient or damaged DNA. *Nat. Protoc.* 8, 737–748.
42. Pajmans, J.L.A., Baleka, S., Henneberger, K., Taron, U.H., Trinks, A., Westbury, M.V., and Barlow, A. (2017). Sequencing single-stranded libraries on the Illumina NextSeq 500 platform. *arXiv*, arXiv:1711.11004. <https://arxiv.org/abs/1711.11004>.
43. Martin, M. (2011). Cutadapt removes adapter sequences from high-throughput sequencing reads. *EMBnet. J.* 17, 10.
44. Li, H., and Durbin, R. (2009). Fast and accurate short read alignment with Burrows-Wheeler transform. *Bioinformatics* 25, 1754–1760.
45. Li, H., Handsaker, B., Wysoker, A., Fennell, T., Ruan, J., Homer, N., Marth, G., Abecasis, G., and Durbin, R.; 1000 Genome Project Data Processing Subgroup (2009). The Sequence Alignment/Map format and SAMtools. *Bioinformatics* 25, 2078–2079.
46. Jónsson, H., Ginolhac, A., Schubert, M., Johnson, P.L.F., and Orlando, L. (2013). MapDamage2.0: fast approximate Bayesian estimates of ancient DNA damage parameters. *Bioinformatics* 29, 1682–1684.
47. Kearse, M., Moir, R., Wilson, A., Stones-Havas, S., Cheung, M., Sturrock, S., Buxton, S., Cooper, A., Markowitz, S., Duran, C., et al. (2012). Geneious Basic: an integrated and extendable desktop software platform for the organization and analysis of sequence data. *Bioinformatics* 28, 1647–1649.
48. Darriba, D., Taboada, G.L., Doallo, R., and Posada, D. (2012). jModelTest 2: more models, new heuristics and parallel computing. *Nat. Methods* 9, 772.
49. Guindon, S., Dufayard, J.-F., Lefort, V., Anisimova, M., Hordijk, W., and Gascuel, O. (2010). New algorithms and methods to estimate maximum-likelihood phylogenies: assessing the performance of PhyML 3.0. *Syst. Biol.* 59, 307–321.
50. Drummond, A.J., Suchard, M.A., Xie, D., and Rambaut, A. (2012). Bayesian phylogenetics with BEAUti and the BEAST 1.7. *Mol. Biol. Evol.* 29, 1969–1973.
51. Lanfear, R., Calcott, B., Ho, S.Y.W., and Guindon, S. (2012). Partitionfinder: combined selection of partitioning schemes and substitution models for phylogenetic analyses. *Mol. Biol. Evol.* 29, 1695–1701.
52. Rambaut, A., Drummond, A.J., Xie, D., Baele, G., and Suchard, M.A. (2018). Posterior summarization in Bayesian phylogenetics using Tracer 1.7. *Syst. Biol.* 67, 901–904.
53. Palombo, M.R., and Ferretti, M.P. (2005). Elephant fossil record from Italy: knowledge, problems, and perspectives. *Quat. Int.* 126–128, 107–136.
54. Palombo, M.R., Mussi, M., Gioia, P., and Cavarretta, G. (2005). Studying proboscideans: knowledge, problems, and perspectives. *Quat. Int.* 126–128, 1–3.
55. Bonfiglio, L., Marra, A.C., and Masini, F. (2000). The contribution of Quaternary vertebrates to palaeoenvironmental and palaeoclimatological reconstructions in Sicily. *Clim. Past Present. Ser. Geol. Soc. London* 181, 171–184.
56. Bonfiglio, L., Esu, D., Mangano, G., Masini, F., Petruso, D., Soligo, M., and Tuccimei, P. (2008). Late Pleistocene vertebrate-bearing deposits at San Teodoro Cave (North-Eastern Sicily): preliminary data on faunal diversification and chronology. *Quat. Int.* 190, 26–37.
57. Masini, F., Petruso, D., Bonfiglio, L., and Mangano, G. (2008). Origination and extinction patterns of mammals in three central Western Mediterranean islands from the Late Miocene to Quaternary. *Quat. Int.* 182, 63–79.
58. Burgio, E., Costanza, M., and Di Patti, C. (2002). I depositi a vertebrati continentali del pleistocene della sicilia occidentale. *Nat. sicil. S. IV* 26, 229–282.
59. Antoniolli, F., Lo Presti, V., Morticelli, M.G., Bonfiglio, L., Mannino, M.A., Palombo, M.R., Sannino, G., Ferranti, L., Furlani, S., Lambeck, K., et al. (2016). Timing of the emergence of the Europe-Sicily bridge (40–17 cal ka BP) and its implications for the spread of modern humans. *Geol. Soc. Spec. Publ.* 411, 111–144.
60. Catalano, G., Modi, A., Mangano, G., Sineo, L., Lari, M., and Bonfiglio, L. (2020). A mitogenome sequence of an *Equus hydruntinus* specimen from Late Quaternary site of San Teodoro Cave (Sicily, Italy). *Quat. Sci. Rev.* 236, 106280.
61. Penkman, K.E.H., Kaufman, D.S., Maddy, D., and Collins, M.J. (2008). Closed-system behaviour of the intra-crystalline fraction of amino acids in mollusc shells. *Quat. Geochronol.* 3, 2–25.
62. Kaufman, D.S., and Manley, W.F. (1998). A new procedure for determining DL amino acid ratios in fossils using reverse phase liquid chromatography. *Quat. Sci. Rev.* 17, 987–1000.
63. Dabney, J., Knapp, M., Glocke, I., Gansauge, M.-T., Weihmann, A., Nickel, B., Valdiosera, C., Garcia, N., Pääbo, S., Arsuaga, J.-L.L., and Meyer, M. (2013). Complete mitochondrial genome sequence of a Middle Pleistocene cave bear reconstructed from ultrashort DNA fragments. *Proc. Natl. Acad. Sci. USA* 110, 15758–15763.
64. Gonzalez-Forbes, G., and Pajmans, J.L.A. (2019). Whole-genome capture of ancient DNA using homemade baits. *Methods Mol. Biol.* 1963, 93–105.
65. Meyer, M., Palkopoulou, E., Baleka, S., Stiller, M., Penkman, K.E.H., Alt, K.W., Ishida, Y., Mania, D., Mallick, S., Meijer, T., et al. (2017). Palaeogenomes of Eurasian straight-tusked elephants challenge the current view of elephant evolution. *eLife* 6, e25413.
66. Korlević, P., Gerber, T., Gansauge, M.-T., Hajdinjak, M., Nagel, S., Aximu-Petri, A., and Meyer, M. (2015). Reducing microbial and human contamination in DNA extractions from ancient bones and teeth. *Biotechniques* 59, 87–93.
67. Westbury, M.V., Hartmann, S., Barlow, A., Preick, M., Ridush, B., Nagel, D., Rathgeber, T., Ziegler, R., Baryshnikov, G., Sheng, G., et al. (2020). Hyena paleogenomes reveal a complex evolutionary history of cross-continental gene flow between spotted and cave hyena. *Sci. Adv.* 6, eaay0456.

68. Ishida, Y., Georgiadis, N.J., Hondo, T., and Roca, A.L. (2013). Triangulating the provenance of African elephants using mitochondrial DNA. *Evol. Appl.* 6, 253–265.
69. Enk, J., Devault, A., Debruyne, R., King, C.E., Treangen, T., O'Rourke, D., Salzberg, S.L., Fisher, D., MacPhee, R., and Poinar, H. (2011). Complete Columbian mammoth mitogenome suggests interbreeding with woolly mammoths. *Genome Biol.* 12, R51.
70. Krause, J., Dear, P.H., Pollack, J.L., Slatkin, M., Spriggs, H., Barnes, I., Lister, A.M., Ebersberger, I., Pääbo, S., and Hofreiter, M. (2006). Multiplex amplification of the mammoth mitochondrial genome and the evolution of Elephantidae. *Nature* 439, 724–727.
71. Rogaev, E.I., Moliaka, Y.K., Malyarchuk, B.A., Kondrashov, F.A., Derenko, M.V., Chumakov, I., et al. (2006). Complete mitochondrial genome and phylogeny of Pleistocene mammoth *Mammuthus primigenius*. *PLoS Biol.* 4, e73.
72. Römpler, H., Rohland, N., Lalueza-Fox, C., Willerslev, E., Kuznetsova, T.V., Rabeder, G., Bertranpetit, J., Schöneberg, T., and Hofreiter, M. (2006). Nuclear gene indicates coat-color polymorphism in mammoths. *Science* 313, 62.
73. Barnes, I., Shapiro, B., Lister, A., Kuznetsova, T., Sher, A., Guthrie, D., et al. (2007). Genetic structure and extinction of the woolly mammoth, *Mammuthus primigenius*. *Curr. Biol.* 17, 1072–1075.
74. Debruyne, R., Chu, G., King, C.E., Bos, K., Kuch, M., Schwarz, C., Szpak, P., Gröcke, D.R., Matheus, P., Zazula, G., et al. (2008). Out of America: ancient DNA evidence for a new world origin of late quaternary woolly mammoths. *Curr. Biol.* 18, 1320–1326.
75. Fellows Yates, J.A., Drucker, D.G., Reiter, E., Heumos, S., Welker, F., Münzel, S.C., Wojtal, P., Láznicková-Galetová, M., Conard, N.J., Herbig, A., et al. (2017). Central European woolly mammoth population dynamics: insights from Late Pleistocene mitochondrial genomes. *Sci. Rep.* 7, 17714.
76. Chang, D., Knapp, M., Enk, J., Lippold, S., Kircher, M., Lister, A., MacPhee, R.D.E., Widga, C., Czechowski, P., Sommer, R., et al. (2017). The evolutionary and phylogeographic history of woolly mammoths: a comprehensive mitogenomic analysis. *Sci. Rep.* 7, 44585.
77. Gillette, D.D., and Madsen, D.B. (1993). The Columbian Mammoth, *Mammuthus columbi*, from the Wasatch Mountains of Central Utah. *J. Paleontol.* 67, 669–680.
78. Drummond, A.J., Nicholls, G.K., Rodrigo, A.G., and Solomon, W. (2002). Estimating mutation parameters, population history and genealogy simultaneously from temporally spaced sequence data. *Genetics* 161, 1307–1320.
79. Stadler, T. (2010). Sampling-through-time in birth-death trees. *J. Theor. Biol.* 267, 396–404.
80. Belluomini, G., and Bada, J.L. (1985). Isoleucine epimerization ages of the dwarf elephants of Sicily. *Geology* 13, 451–452.
81. Blackwell, B., Rutter, N.W., and Debénath, A. (1990). Amino acid racemization in mammalian bones and teeth from La Chaise de Vouthon (Charente), France. *Geoarchaeology* 5, 121–147.
82. Penkman, K.E.H., Preece, R.C., Bridgland, D.R., Keen, D.H., Meijer, T., Parfitt, S.A., et al. (2013). An aminostratigraphy for the British Quaternary based on *Bithynia opercula*. *Quat. Sci. Rev.* 61, 111–134.
83. Oakley, D.O.S., Kaufman, D.S., Gardner, T.W., Fisher, D.M., and Vanderleest, R.A. (2017). Quaternary marine terrace chronology, North Canterbury, New Zealand, using amino acid racemization and infrared-stimulated luminescence. *Quat. Res.* 87, 151–167.
84. Dickinson, M.R. (2018). Enamel Amino Acid Racemisation Dating and its Application to Building Proboscidean Geochronologies (University of York), PhD thesis.
85. Wehmiller, J.F., Stecher, H.A., York, L.L., and Friedman, I. (2000). The thermal environment of fossils: effective ground temperatures at aminostratigraphic sites on the U.S. Atlantic Coastal Plain. In *Perspectives in Amino Acid and Protein Geochemistry*, G.A. Goodfriend, M.J. Collins, M.L. Fogel, S.A. Macko, and J. Wehmiller, eds. (Oxford University Press), pp. 219–250.
86. Ambrosetti, P. (1967). Cromerian fauna of the Rome area. *Quaternaria* 9, 1–17.
87. Stuart, A.J. (1982). *Pleistocene Vertebrates in the British Isles* (Longman).
88. Zalasiewicz, J.A., Mathers, S.J., Gibbard, P.L., Peglar, S.M., Funnell, B.M., Catt, J.A., Harland, R., Long, P.E., and Austin, T.J.F. (1991). Age and relationships of the Chillesford Clay (early Pleistocene: Suffolk, England). *Philos. Trans. R. Soc. Lond., B* 333, 81–100.
89. Hamblin, R.J.O., Moorlock, B.S.P., Booth, S.J., Jeffery, D.H., and Morigi, A.N. (1997). The Red Crag and Norwich Crag formations in eastern Suffolk. *Proc. Geol. Assoc.* 108, 11–23.
90. Lister, A.M. (1998). The age of Early Pleistocene mammal faunas from the “Weybourne Crag” and Cromer Forest-bed Formation (Norfolk, England). *Meded. Ned. Inst. voor Toegepaste Geowetenschappen* 60, 271–280.
91. Brassey, C.A. (2016). Body-mass estimation in paleontology: a review of volumetric techniques. *Paleontol. Soc. Pap.* 22, 133–156.
92. Lister, A.M., and Stuart, A.J. (2010). The West Runton mammoth (*Mammuthus trogontherii*) and its evolutionary significance. *Quat. Int.* 228, 180–209.
93. Christiansen, P. (2004). Body size in proboscideans, with notes on elephant metabolism. *Zool. J. Linn. Soc.* 140, 523–549.

STAR★METHODS

KEY RESOURCES TABLE

REAGENT or RESOURCE	SOURCE	IDENTIFIER
Chemicals, peptides, and recombinant proteins		
Guanidine hydrochloride	Roth	Cat#0037.1
QIAGEN MinElute kit	QIAGEN	Cat#28004
Sodium hypochlorite, reagent grade	Sigma Aldrich	Cat#425044
Sodium hypochlorite 12 % Cl ₂ in aqueous solution	VWR Chemicals	CAS No: 7681-52-9
Hydrochloric acid S.G. 1.18 (~36 %)	Fisher Scientific	CAS No: 7647-01-0
Analytical reagent grade Potassium hydroxide	Fisher Scientific	CAS No: 1310-58-3
Ethylenediaminetetra-acetic acid	VWR Chemicals	CAS No: 60-00-4
HPLC grade Sodium acetate trihydrate	Fisher Scientific	CAS No: 6131-90-4
Sodium azide	VWR Chemicals	CAS No: 26628-22-8
HPLC grade Methanol	Fisher Scientific	CAS No: 67-56-1
Critical commercial assays		
D1000 Screen Tape (Tapestation2200)	Agilent	Cat#5067-5582
dsDNA HS Assay Kit (Qubit 2.0)	Thermofisher	Cat#Q32851
Deposited data		
EM9/GP4 mitochondrial genome sequence	This paper	MK034300
Oligonucleotides		
CL9 extension primer: GTGACTGGAGTTCAG ACGTGTGCTCTTCCGATCT	41	Sigma Aldrich
Double-stranded adaptor	41	Sigma Aldrich
Strand 1 (CL53): CGACGCTCTTC-ddC (ddC = dideoxycytidine)		
Strand 2 (CL73): [Phosphate] GGAAGAGCGTCGTGTAGGGAAAGAGT*G*T*A (* = phosphothioate linkage)		
CL78: AGATCGGAAG[C3Spacer] ₁₀ [TEG-biotin] (TEG = triethylene glycol spacer)	41	Sigma Aldrich
P5 indexing primer: AATGATACGGCGACCACC GAGATCTACACnnnnnnnnACACTCTTCCCTA CACGACGCTCTT	41	Sigma Aldrich
P7 indexing primer: CAAGCAGAAGACGGCA TACGAGATnnnnnnnnGTGACTGGAGTTCAG ACGTGT	41	Sigma Aldrich
IS7 amplification primer: ACACTCTTCCCT ACACGAC	41	Sigma Aldrich
IS8 amplification primer: GTGACTGGAGTTC AGACGTGT	41	Sigma Aldrich
CL72 R1 sequencing primer: ACACTCTTCC CTACACGACGCTCTTCC	41	Sigma Aldrich
Gesaffelstein index 2 sequencing primer: GGAAGAGCGTCGTGTAGGGAAAGAGTGT	42	Sigma Aldrich
Software and algorithms		
Cutadapt v1.10	43	https://cutadapt.readthedocs.io/en/stable/
BWA v0.7.8	44	http://bio-bwa.sourceforge.net/
Samtools v1.1.19	45	https://sourceforge.net/projects/samtools/files/samtools/
MarkReadsByStartEnd.jar	N/A	https://github.com/dariober/Java-cafe/tree/master/MarkDupsByStartEnd

(Continued on next page)

Continued

REAGENT or RESOURCE	SOURCE	IDENTIFIER
MapDamage v2.0.2	46	https://ginolhac.github.io/mapDamage/
Geneious v10.1.3	47	https://www.geneious.com/
jModelTest v2.1.4	48	https://github.com/ddarriba/jmodeltest2
PhyML v3.3.3	49	https://github.com/stephaneguindon/phyml
BEAST v1.8.2	50	https://beast.community/
Partitionfinder v1.1.1	51	https://github.com/brettc/partitionfinder
Tracer v1.5.0	52	http://tree.bio.ed.ac.uk/software/tracer/
Treeannotator v1.8.2	NA	https://beast.community/treeannotator
FigTree v1.4.2	NA	http://tree.bio.ed.ac.uk/software/figtree/

Other

Proteinase K	Promega	Cat#V3021
Zymo-spin V column extension reservoir	Zymo	Cat#C1016-50
Circligase II	Biozym	Cat#131402(CL9021K)
Endonuclease VIII	NEB	Cat#A0299S
Uracil-DNA glycosylase (Afu UDG)	NEB	Cat#M0279S
FastAP	Thermo Fisher	Cat#EF0651
Dynabeads MyOne C1	Thermo Fisher	Cat#65001
Bst 2.0 polymerase	NEB	Cat#M0537S
T4 DNA Polymerase	Thermo Fisher	Cat#EP0061
Buffer Tango (10x)	Thermo Fisher	Cat#BY5
T4 DNA ligase	Thermo Fisher	Cat#EL0011
Accuprime Pfx	Thermo Fisher	Cat#12344024
PEG-4000	Thermo Fisher	Cat#EP0061
Klenow fragment of DNA polymerase I	Thermo Fisher	Cat#EP0051
SYBR green PCR MasterMix	Thermo Fisher	Cat#4309155

RESOURCE AVAILABILITY

Lead contact

Requests for further information should be directed to and will be fulfilled by the Lead Contact, Sina Baleka (sina.baleka@gmail.com).

Materials availability

This study did not generate new unique reagents.

Data and code availability

The mitochondrial genome sequence for the Puntali elephant sample (labcode EM9/GP4) has been deposited in GenBank: MK034300.

EXPERIMENTAL MODEL AND SUBJECT DETAILS

Samples

A total of 11 dwarf elephant samples were processed for palaeogenetic analysis from four sites (San Teodoro, Puntali, Zà Minica, and San Ciro), consisting of teeth, postcranial elements and petrous bones (Table S2). All specimens analyzed belong to the G.G. Gemmellaro collection located in the geological museum in Palermo, Italy, and were assigned to “*Palaeoloxodon (Elephas) mnaidriensis*”. After initial screening (see section “Bioinformatic procedures”), library EM9/GP4, obtained from the petrous bone of skull GP4 from Puntali Cave, was selected for further analysis.

Chiral amino acid analysis was undertaken on 13 elephantid teeth, 9 from Spinagallo cave and 4 from Puntali cave (including from skull GP4; Table S1).

Taxonomy of Sicilian dwarf elephants

Although only two Sicilian dwarf elephant taxa are described in the main text (*Palaeoloxodon falconeri* and *P. cf. mnaidriensis*), debate over the taxonomy and systematics of Sicilian dwarf elephants is ongoing. There are at least two further taxa suggested: one

intermediate in size between *P. falconeri* and the Puntali Cave material, which may pre-date and thus potentially be ancestral to *P. falconeri*,^{13,53} and a larger-sized taxon, sometimes attributed to a large form of *P. cf. mnaidriensis*.⁵⁴ The faunal assemblages of the Sicilian Pleistocene can be arranged into five biochrons named “Faunal Complexes” (FC; absolute age-ranges for the correlated sub-epochs are provided as a guide):^{55–57} “Monte Pellegrino FC” (Early Pleistocene, ca. 2.58–0.77 Ma), “*Elephas falconeri* FC” (early Middle Pleistocene, ca. 0.77–0.42 Ma), “*Elephas mnaidriensis* FC” (late Middle-early Late Pleistocene, ca. 0.42–0.07 Ma), “San Teodoro-Pianetti FC” (late Late Pleistocene, ca. 0.07–0.012 Ma) and “Castello FC” (Late Glacial, ca. 0.015–0.012 Ma).

While *P. cf. mnaidriensis* is identified in both the *Elephas mnaidriensis* FC and in the San Teodoro-Pianetti FC, given the potential of multiple dwarfing events and the homoplastic nature of insular dwarfism, it is possible that *P. cf. mnaidriensis* represents a “dustbin” taxon lumping all moderately-dwarfed *Palaeoloxodon*. Furthermore, comparisons with type material of *P. mnaidriensis* from Malta indicate that the current attribution of material to *P. cf. mnaidriensis* on Sicily is incorrect, and that it in fact represents a distinct, as yet unnamed larger-sized taxon.¹³ Additionally, it is unclear whether the younger San Teodoro-Pianetti FC dwarf elephants represent a later colonization/dwarfing event, or persistence of *P. cf. mnaidriensis* from the preceding faunal complex. Therefore, and even though the elephants from Puntali cave have often been described as *P. (cf.) mnaidriensis*, we refer to it as “Puntali elephant.”

Faunal complex correlations and age of sample

Puntali Cave (*Grotta dei Puntali*) is a karstic cavity situated 90 m above sea level in the Carini region of north-western Sicily.¹ Site chronology and the age of the elephant remains are complicated by a lack of clear provenance for the mammalian fossil material and a paucity of reliable direct dates on specimens. Elephant material was recorded from both layers 2 and 3, and it cannot be established from which of these layers the sequenced Puntali elephant sample derives. Elephant material from Puntali Cave can all be attributed to the same size class of dwarf elephant (generally referred to *P. cf. mnaidriensis*) as variation is within the range expected for a single species of elephant.¹³ Without stratigraphical provenance of fossil material, finer scale size-change patterns cannot be established. The elephant material derived from layers 2 and 3 can thus be treated as a time-averaged fossil assemblage constrained by the first and last appearance datum of *P. cf. mnaidriensis* material on Sicily. The presence of *Hippopotamus* alongside elephants in layer 3 supports attribution to the *E. mnaidriensis* FC, and this is generally taken to be the faunal complex association for Puntali Cave fossil elephants.⁵⁸ However, the faunal composition of layer 2 is non-diagnostic and could be attributed to either the *E. mnaidriensis* FC or the younger San Teodoro-Pianetti FC.

Fossils attributed to the *E. mnaidriensis* FC have been dated to between 88.2 ka ± 19.5 (Early Uptake, EU, model) and 146.8 ± 28.7 ka (Linear Uptake, LU, model) on the basis of Electron Spin Resonance (ESR) dating of elephant and hippo tooth enamel from Contrada Fusco, Siracusa.²⁴ This provides the first appearance date for *P. cf. mnaidriensis* on Sicily, with an upper bound age (including error) of 175.5 ka, although the true age of the Contrada Fusco samples likely lies in between the EU and LU ages (E. Rhodes, personal communication).²⁴ The San Teodoro-Pianetti FC is estimated at 70–20 ka BP,⁵⁷ with some elephant remains from San Teodoro Cave attributed to this faunal complex dated to before 32 ± 4 ka on the basis of U-Th dates on overlying calcitic material,⁵⁶ while others are dated to 21–23 ka BP on the basis of radiocarbon-dated, stratigraphically associated *Equus hydruntinus* material.^{59,60} This provides the last appearance date for *P. cf. mnaidriensis* on Sicily. Thus, the first and last appearance dates are 146.8 ± 28.7 ka and 21–23 ka BP, respectively. However, the non-finite radiocarbon date excludes ages younger than 50 ka for our Puntali elephant sample.

METHOD DETAILS

Laboratory procedures

Radiocarbon dating

Sample GP4 was radiocarbon dated at the Oxford Radiocarbon Accelerator Unit (ORAU) under the reference C14/5236. The sample contained enough collagen for dating, but the age of the sample was found to be beyond the range of carbon dating (> 46,500 radiocarbon years, OxA-38261). We therefore used 50 ka as youngest possible sample age in our calculations.

Amino acid geochronology

Enamel chips were powdered with an agate pestle and mortar, and prepared using modified procedures from Penkman,⁶¹ but optimized for enamel, using a bleach time of 72 hours to isolate the intra-crystalline protein.²⁰

Approximately 30 mg of powdered enamel was weighed into a 2 mL plastic microcentrifuge tube (Eppendorf), and NaOCl (12%, 50 μL mg^{−1} of enamel) was added. Samples were exposed to bleach for 72 h and were continuously rotated to ensure complete exposure.^{20,61} The bleach was pipetted off and the powdered enamel was washed five times with HPLC-grade water. A final wash with methanol was used to react with any remaining bleach, before being left to air dry overnight.

Powdered enamel samples were accurately weighed into two fractions: a free amino acid (FAA) and a total hydrolysable amino acid (THAA) fraction. THAA samples were hydrolyzed in HCl (7 M, 20 μL mg^{−1}) and heated in a sterile sealed glass vial at 110 °C for 24 h. Vials were purged with N₂ to prevent oxidation. The acid was removed by centrifugal evaporation and THAA samples were re-dissolved in HCl (1 M, 20 μL mg^{−1}). FAA samples were demineralized in HCl (1 M, 25 μL mg^{−1}) in a sterile 0.5 mL microcentrifuge tube (Eppendorf) and sonicated for 10 min. To remove the high concentrations of phosphate ions, KOH (28 μL mg^{−1}) was added to both the FAA and THAA samples. Upon addition of KOH, a mono-phasic cloudy solution formed. The solution was centrifuged at 13,000 rpm for 10 min and a clear supernatant formed above a gel. The supernatant was removed and dried by centrifugal evaporation.

All samples were rehydrated in 30 μ L of a solution containing HCl (0.01 M) and sodium azide (1.5 mM) as well as an internal standard, L-homo-arginine (0.01 mM) that acted as standard for quantification of amino acids. Analysis of chiral amino acid pairs was achieved using an Agilent 1100 series HPLC fitted with a HyperSil C18 base deactivated silica column (5 μ m, 250 \times 3 mm) and fluorescence detector, using a method modified from that outlined by Kaufman and Manley.⁶² The column temperature was controlled at 25°C and a tertiary solvent system containing sodium buffer (23 mM sodium acetate trihydrate, 1.5 mM sodium azide, 1.3 μ M EDTA, adjusted to pH 6.00 \pm 0.01 with 10 % acetic acid and sodium hydroxide), acetonitrile and methanol was used. The ratios of amino acid D- and L- isomers (D/L value) were calculated based on peak areas.

Ancient DNA laboratory methods

All pre-amplification steps were carried out in the dedicated ancient DNA facilities at the University of Potsdam, including negative controls for both extraction and library preparation. In a first round of screening, \sim 50 mg of bone powder per sample were produced using a mikrodismembrator (Retsch) at a frequency of 30 Hz for 10 s. DNA was extracted following a protocol optimized for highly fragmented DNA.⁶³ In brief, bone powder was incubated overnight in 1 mL extraction buffer (0.45 M EDTA, 0.25 mg/mL Proteinase K) at 37°C under constant rotation. Remaining undigested material was pelleted using centrifugation and the supernatant was transferred into 13 mL of binding buffer (5 M guanidine hydrochloride, 40% isopropanol, 0.05% Tween-20, and 90 mM sodium acetate). This mix was passed through QIAGEN MinElute columns fitted with a reservoir (Zymo-Spin V). PE buffer (QIAGEN) was used in two subsequent wash steps followed by a dry spin of 1 min at 13,000 rpm to remove remaining PE buffer. The purified DNA was eluted in TET buffer (10 mM Tris-HCl, 1 mM EDTA, 0.05% Tween-20) using a two-step approach each time adding 12.5 μ L TET.

Single-stranded Illumina sequencing libraries were prepared from the extracts following a published protocol.⁴¹ To remove uracil residues, which can accumulate in high frequency in ancient DNA as a result of cytosine deamination, samples were treated with uracil-DNA glycosylase (UDG) and Endonuclease VIII prior to library preparation in a 44 μ L reaction containing 1.8x CircLigase buffer II, 4.5 mM MnCl₂, 0.02 U/ μ L UDG, and 0.11 U/ μ L Endonuclease VIII. One Unit of FastAP was used to remove residual phosphate groups and the DNA was denatured at 95°C for 2 min. Adaptor CL78 was ligated to the 3' end of the now single-stranded DNA in a 80 μ L reaction containing 20% (vol/vol) PEG-4000, 0.125 mM CL78, and 2.5 U/ μ L CircLigase II, which was incubated overnight at 60°C. The DNA was immobilised on streptavidin covered magnet beads (Dynabeads MyOne C1) and extension primer CL9 was annealed to the complementary CL78 adaptor. To fill in the second strand, Bst 2.0 polymerase was used in a 50 μ L reaction containing 1x isothermal amplification buffer, 250 mM of each dNTP, 2 mM CL9 extension primer, and 0.48 U/ μ L Bst 2.0 polymerase. For blunt-end repair, a 100 μ L reaction with the following reagents was used: 1x Buffer Tango, 0.025% (vol/vol) Tween 20, 100 mM of each dNTP, and 0.05 U/ μ L T4 DNA polymerase. The second, double-stranded adaptor (CL53/CL73) was now ligated to the blunt-ended molecules in a 100 μ L reaction containing 1x T4 DNA ligase buffer, 5% (vol/vol) PEG-4000, 0.025% (vol/vol) Tween 20, 2 mM double-stranded adaptor, and 0.1 U/ μ L T4 DNA ligase. Again, using 95°C for 1 min to denature the DNA molecule, the strand complementary to the original single-stranded molecule was eluted in 25 μ L of TET buffer. Libraries were amplified and indexed (using unique indices within both P5 and P7 adapters) in 80 μ L reactions containing 1x AccuPrime Pfx reaction mix, 10 mM each of P5 and P7 indexing primers, and 0.025 U/ μ L AccuPrime Pfx polymerase. The optimal number of cycles was determined by qPCR prior to amplification in 10 μ L reactions with the following reagents: 1x SYBR green qPCR master mix, 0.2 mM each of IS7 and IS8 amplification primers, and 1 μ L of a 1:20 dilution of the unamplified library. The amplified and indexed libraries were then quantified on a TapeStation 2200 (Agilent) using a D1000 screen tape and reagents, and on a Qubit 2.0 Fluorometer (Fisher) using the dsDNA HS Assay kit. To assess DNA preservation and levels of contamination, samples were sequenced on an Illumina NextSeq 500 in 75 bp single-end mode using the custom CL72 R1 primer⁴¹ and the Ge-saffelstein custom index 2 sequencing primer,⁴² generating 1–2 million reads per sample (Table S2).

Libraries were then enriched for mitochondrial DNA by performing two rounds of in-solution hybridization capture.⁶⁴ The same capture baits as in previous work on *P. antiquus* were used.⁶⁵ Only sample EM9/GP4 yielded a usable amount of mitochondrial DNA after capture (Table S2). To improve the mitochondrial coverage, ten parallel extractions (\sim 25 mg bone powder each) were performed with an additional pre-treatment with 1 mL of 1% sodium hypochlorite for 15 min.⁶⁶ Library preparation, in-solution capture and sequencing were carried out as described above, this time generating roughly 2–4 million reads per library (Table S2).

QUANTIFICATION AND STATISTICAL ANALYSIS

Bioinformatic procedures

Sequence processing

Cutadapt 1.10⁴³ was used to trim adaptor sequences and low quality bases (< Q30). Untrimmed reads were discarded. For each library, an individual minimum length cut-off was determined as described previously (Table S2).⁶⁷ Trimmed reads were mapped to the nuclear genome of the African savanna elephant *L. africana* (loxAfr3, GenBank: GCA_000001905.1) and the mitochondrial genomes of *Palaeoloxodon antiquus* (GenBank: NC_035230.1) and *L. africana* (GenBank: NC_000943) using default parameters in BWA 0.7.8 (Table S2).⁴⁴ Reads with a mapping quality below 30 were removed using Samtools 0.1.19.⁴⁵ Duplicate reads (reads with the same start and end coordinates) were identified using the java program MarkDuplicatesByStartEnd.jar (<https://github.com/dariober/Java-cafe/tree/master/MarkDupsByStartEnd>) and removed. Cytosine deamination patterns and read length distribution were calculated using MapDamage 2.0.2.⁴⁶ The mean fragment length was 29.55 bp, and deamination at the 5' terminal nucleotide was 29% (Figure S1). For each mitochondrial reference, a consensus sequence was called using Geneious 10.1.3⁴⁷ with 85% majority rule for

base calling and minimum coverage of 3x (Figure S1). No differences were observed between the two consensus sequences, suggesting no impact of reference bias. The more complete consensus sequence recovered from mapping to the straight-tusked elephant reference covers a length of 16,106 bp (approximately 95.5% complete) with an average read depth of 61x.

Maximum likelihood analysis

The consensus sequence for each mitochondrial reference was aligned with 33 other proboscidean mitogenomes (Figure S1) using MUSCLE as implemented in Geneious, with a maximum number of six iterations. The D-loop was removed from the alignment resulting in an alignment of 15,437 bp length. The most appropriate substitution model was selected for each alignment using jModelTest 2.1.4⁴⁸ under the Bayesian Information Criterion (BIC). The program PhyML 3.3.3⁴⁹ was used to calculate a maximum-likelihood phylogenetic tree with 100 bootstrap replications using the selected TrN+I+G substitution model. The resulting phylogenies place the Puntali elephant as sister lineage to the straight-tusked elephants from Neumark-Nord with 100% bootstrap support in all cases, ruling out any impact of reference bias on the phylogenetic placement of the Puntali elephant (Figure S2D). Therefore, the more complete consensus sequence recovered from mapping to the straight-tusked elephant reference was used in all further analyses.

We also analyzed a larger dataset including 675 partial mitochondrial sequences of 4258 bp length (ranging from partway through ND5 to partway through the control region). The dataset contained 653 African elephant sequences previously published⁶⁸ (GenBank: JQ438119–JQ438771), 16 complete mitochondrial *Loxodonta* sequences (GenBank: NC_000934, NC_020759, AB443879, DQ316069, JN673263, KJ5574243, KJ557424, KY616974 – KY616981), four *P. antiquus* sequences (GenBank: KY499555–KY499558) as well as our sequence from Puntali and one *E. maximus* sequence to serve as outgroup (GenBank: NC_005129). Identical sequences were collapsed, resulting in 122 unique sequences. Phylogenetic tree reconstruction was performed as described above: sequences were aligned using MUSCLE and jModelTest was used to select the optimal substitution model for the alignment (HKY+I+G). Phylogenetic reconstruction was performed using PhyML with 100 bootstrap replications (Figure S3).

Calibrated Bayesian analysis

To estimate the divergence time between the Puntali elephant and the European straight-tusked elephant (*P. antiquus*), Bayesian analyses were performed in BEAST 1.8.2.⁵⁰ We created a new alignment using all available mitochondrial genomes of *Loxodonta africana* (GenBank: NC_000934, AB443879, DQ316069, KY616974, KY616977, KY616982); *Loxodonta cyclotis* (GenBank: NC_020759, JN673263, KJ5574243, KJ557424, KY616975, KY616976, KY616978 – KY616981); *Palaeoloxodon antiquus* (GenBank: KY499555 – KY499558); and *Elephas maximus* (GenBank: NC_005129, AJ428946, EF588275); as well as three mitochondrial genomes for each of the three clades of *Mammuthus primigenius* (Clade 1: GenBank: JF912200, NC_007596, DQ316067; Clade 2: GenBank: KX176755, KX176751, KX027533; Clade 3: GenBank: KX027531, MF579937, KX176773); the reference sequence for *Mammuthus columbi* (GenBank: NC_015529); and our sequence for the Puntali elephant. As before, the D-loop was removed and sequences were aligned using MUSCLE with a maximum of 6 iterations. Partitionfinder 1.1.1⁵¹ was used to find an optimal set of partitions and substitution models under the Bayesian information criterion from all possible combinations of rRNAs, tRNAs and the individual codon positions of protein coding genes, using the greedy search algorithm and linked branch lengths and only considering those models available in BEAST. This resulted in a six partition scheme. We performed two BEAST analyses using a Bayesian skyline coalescent tree prior and either 50 ka or 175.5 ka for the age of the Puntali elephant, respectively. All analyses used lognormal relaxed clock models for each partition, with uninformative uniform priors ($0 - 2.0 \times 10^{-7}$ substitutions/site/year) on the mean substitution rates. Ancient samples in the alignment were fixed at their calibrated radiocarbon or estimated ages from their respective publications: GenBank: JF912200 – 44,964 years,⁶⁹ NC_007596 – 14,056 years,⁷⁰ DQ316067 – 37,068 years,⁷¹ KX176755 – 42,960 years,⁷² KX176751 – 47,022 years,⁷³ KX027533 – 44,806 years,⁷⁴ KX027531 – 42,815 years,⁷⁴ MF579937 – 31,666 years,⁷⁵ KX176773 – 43,960 years,⁷⁶ NC_015529 – 13,082 years,⁷⁷ 120 ka for *P. antiquus* from Neumark-Nord (GenBank: KY499555 – KY499557) and 240 ka for *P. antiquus* from Weimar-Ehringsdorf (GenBank: KY499558).⁶⁵ As node calibrations, we used the divergence of Asian elephants and mammoths at 5.6 Ma (normal prior with a mean of 5.6 Ma and a standard deviation of 850 ka), and the divergence of African (*Loxodonta* and *Palaeoloxodon*) and Eurasian elephants (*Elephas* and *Mammuthus*) at 7.5 Ma (normal prior with a mean of 7.5 Ma and a standard deviation of 900 ka), following the fossil calibrations used previously.²⁸ Monophyly was enforced for each of the calibrated nodes. The MCMC chain was run for 200 million generations. Convergence and adequate sampling (ESS > 200) of all parameters were verified in Tracer v1.5.0.⁵² The first 25% of trees were removed as burn-in, and the maximum clade credibility trees obtained from the posterior sample, with nodes heights scaled to the median of the posterior sample, using TreeAnnotator, and visualized in FigTree. As population structuring among and within species may violate the assumptions of the Bayesian skyline model, we replicated our analyses using a Birth-Death Serially Sampled speciation tree prior^{78,79} and a subsampled dataset including a single representative of each species (GenBank: KY499555, MF579937, NC_005129, NC_015529, JN673263, NC_000934, and the Puntali elephant). All other model specifications and priors were as described for the Bayesian skyline analyses. All BEAST input xml files are available upon request.

Intra-crystalline protein degradation dating of enamel

Early attempts at amino acid racemisation (AAR) dating on enamel from a Puntali Cave elephant molar gave ages of 180 ± 45 ka,⁸⁰ which was recalculated to 142 ± 28 ka following new calibration dates for Isernia La Pineta.¹³ However, the original AAR methodology is likely to have sampled open-system protein, which would compromise the geochronological information for both absolute and relative dating.⁸¹

More recent amino acid geochronology studies have isolated the intra-crystalline fraction of calcium carbonate based biominerals, such as shells, which provides a closed-system repository enabling amino acid degradation to be used as an accurate indicator of

age.^{82,83} Further developments in the preparative method of calcium phosphate based biominerals have enabled the expansion of the intra-crystalline protein decomposition (IcPD) technique to mammalian remains.²⁰ In a closed system, the extent of racemisation can be used to infer the relative ages of samples with similar temperature histories, as the progress of the reaction is only dependent on temperature and time. It has been shown that a fraction of amino acids that exhibits closed system behavior can be isolated from elephantid tooth enamel, making it suitable for use as a tool for relative age estimation.^{20,84}

The enamel IcPD data from Puntali was compared to a number of other *P. cf. mnaidriensis* and *P. falconeri* samples from other Sicilian sites. All the *P. cf. mnaidriensis* samples come from karstic sites similar to that of the Puntali specimen, as does the Spinagallo *P. falconeri*, and are therefore likely to have experienced similar effective diagenetic temperatures.⁸⁵ Spinagallo was independently dated to ~230-350 ka by optically stimulated luminescence and uranium-series²¹ and is a karstic cave in the Hyblean Plateau 110 m above sea level, west of Syracuse.⁸⁶ The levels of racemisation in enamel from the Puntali elephant skull GP4, as well as other specimens from Puntali, are significantly lower than those observed from Spinagallo and other sites with *P. falconeri* (Figure S1; Table S1). *p* values for the student's 2-tailed *t* test (for normally distributed data) and Mann-Whitney tests (for non-normal data) for Asx, Glx, Ala and Phe D/L in both FAA and THAA fractions show that the extent of racemisation is statistically different between the two sites at a < 0.1% confidence level. All *P. cf. mnaidriensis* samples cluster together, supporting a younger age for this larger dwarf elephant form. Therefore, the enamel IcPD values obtained for the Puntali samples analyzed support a Late Middle to Late Pleistocene age. Given the significant distance between the two clusters of data, an older (~200 ka) age for the Puntali material is unlikely, but as only a limited comparative dataset is available, the IcPD is not currently able to distinguish between other possible ages for the Puntali elephant specimen.

IcPD is dependent on time and temperature, with the rate of IcPD being greater at higher temperatures. Therefore, some confirmation of likely age can be obtained by comparing the more limited Sicilian dataset to the larger dataset of elephantid material from the UK. Sicily is south of the UK and therefore the mean temperature will also have been higher during the Pleistocene. Due to these higher temperatures the rates of racemisation are expected to be greater.²⁰ This is supported by comparing the extent of racemisation in the Sicilian material from Spinagallo (230-350 ka; Table S1), which is generally greater than that of material from the Norwich Crag formation (1.9-2.2 Ma; Table S1).⁸⁷⁻⁹⁰ The Sicilian material from Puntali Cave shows similar IcPD to material from Crayford, UK, which has been correlated with the MIS 7/6 boundary (ca. 200 ka; Table S1).^{22,23} Therefore, given the substantially greater rates of racemisation in Sicily, it is unlikely that the Puntali material would be of comparable age to Crayford, which again supports an age estimate younger than 200 ka for the Puntali sample.

Body size estimation

We consider change in the most widely used metrics of body size in elephants, shoulder height (SH; m) and body mass (BM; kg), between Puntali Cave dwarf elephants and their putative full-sized mainland ancestral species, the European straight-tusked elephant (*P. antiquus*). Body size for extinct species is reconstructed from skeletal remains using information gleaned from closely related extant species, with potential error introduced from (i) incompleteness of the fossil skeletal material available, or (ii) allometric differences in body proportions between fossils and extant model species. In addition, the mass of an individual may not be representative of a population as a whole, especially in sexually dimorphic taxa such as elephants. Volumetric estimation methods have been shown to perform better than estimates based on linear regression, mitigating issues relating to (ii);⁹¹ however, the only volumetric mass estimates available for *P. antiquus* and Puntali Cave dwarf elephants (BM = 13 t, and SH = 4 m, for "Grade I" (= "average-sized") males; and BM = 1.7 t, and SH = 2 m for Puntali Cave elephants, respectively)³ do not have the associated raw or summary statistical data needed to calculate evolutionary rate in Haldanes. We instead estimated body mass and shoulder height from V.L.H.'s own data on male *P. antiquus* and Puntali Cave material, combined with new data (Table S3),²⁵ using linear allometric equations.^{92,93}

$$\text{Shoulder Height (SH, mm)} = (183.631 + 2.8744 \times \text{humerus TL}) \quad (\text{Equation 1})$$

$$\text{Log10 Body Mass (BM, kg)} = -4.15 + 2.64 \times \text{log10 humerus TL} \quad (\text{Equation 2})$$

where humerus TL is the greatest length of the humerus measured in mm on complete, fully or almost fully-grown specimens (aged > 20 African Elephant Years on the basis of associated dental material, or with at least one epiphyses fusing). While allometric approaches may introduce some error versus the volumetric "gold-standard" methodology, for *P. antiquus* differences in BM estimation between Christiansen⁹³ and Larramendi³ have been shown to be relatively small (4.68%).³ Nevertheless, our mean BM (10.1 t) and SH (3.7 m) estimates for *P. antiquus* are lower than estimated before,³ but similar for Puntali Cave, perhaps reflecting sampling differences and age-selection. Rather than a true mean value, the estimates for "average-sized" individuals in Larramendi³ represent a maximum size for both (A. Larramendi, personal communication to A.M.L. and V.L.H., 2020).²⁵

Given that straight-tusked elephants (and thus probably also their dwarf descendants) are sexually size-dimorphic, we limited our full-size dataset to probable male *P. antiquus* specimens given the likelihood that the Puntali Cave specimens were also male (unimodal distribution of limb bone size and absolute levels of observed variation is consistent with a single size class (and therefore sex),¹³ while the pronounced parieto-occipital crest on the Puntali Cave skulls suggests that sex was male). This could lead to an overestimate of size change during insular dwarfism if our sex-identification for Puntali Cave is incorrect. Conversely, however, a pooled sex sample would potentially underestimate the degree of size change, and we consider our approach sufficiently

conservative given the weight of evidence in support of a male assemblage, and the lower BM and SH estimates produced by us versus the widely-cited values obtained by Larramendi³ for “average” *P. antiquus* males.

Evolutionary rates

We calculated evolutionary rates in haldanes (H; one haldane corresponds to a change in a trait by one standard deviation per generation)³⁹ for shoulder height-, and body mass-, estimated from total humerus length of the Puntali elephants and mainland straight-tusked elephant (Table S3) for the longest (352 ka) and shortest (1.3 ka) dwarfing time intervals (Table 1), respectively. Gingerich’s method corrects for sampling interval,⁴⁰ so despite encompassing a wide range of time over which dwarfing may have occurred (from 352 ka to 1.3 ka), all calculated rates (range LogH (SH): -1.91 to -3.32 ; range LogH (BM): -2.08 to -3.16) fall within other observed palaeontological evolutionary rates, at the upper (i.e., fast) end of the range (Figure 8 in Gingerich).⁴⁰